Voltage Unbalance Management for High-speed Railway Considering the Impact of Large-scale Wind Farm

Yinyu Chen, *Student Member, IEEE*, Minwu Chen, *Member, IEEE*, Zhongbei Tian, Yuanli Liu

Abstract—**The worse voltage unbalance (VU) problems are aroused by single-phase 25-kV traction power supply systems (TPSSs) of high-speed railways (HSRs) in three-phase power grid, especially when connected to a weak remote grid which is around a number of large-scale wind farms. Implementing VU management for HSRs, including limit government and compensation for VU, is an important approach to ensure the network operating securely. In this paper, to portray the power performance of WPGs under the unbalance condition, a complex voltage unbalance factor (CVUF) is introduced to establish a clear mathematical relationship between the VU and output power of wind power generator (WPG). Furthermore, employing the consumption capability of WPGs for unbalance power, a VU limit pre-assessment approach for HSR is developed based on the IEC/TR 61000-3-13, which provides an objective for VU compensation of TPSS. To reach the allocated VU limit and optimize the traction substation (TSS) capacity, establishing a uniform VU propagation model that takes in account of the TPSS, wind farm and grid, a novel computation approach is proposed to provide a reference compensation current to TPSS. Compared with initial compensation result, a TSS capacity can be reduced by 22%. The effectiveness of the VU limit pre-assessment method and compensation approach for TPSS is verified by a case study.**

***Index Terms*—high-speed railway, voltage unbalance, VU management, wind farm.**

ABBREVIATION

CCUF	Complex current unbalance factor.
CVUF	Complex voltage unbalance factor.
DFIG	Double-fed induction generator.
EMU	Electric multiple unit.
HSR	High-speed railways.
PCC	Point of common coupling.
PFC	Power flow controller.
RPC	Railway power conditioner.
TPSS	Traction power supply system.
TSS	Traction substation.
TT	Traction transformer.
VU	Voltage unbalance.
WPG	Wind power generator.

This work was supported in part by the National Natural Science Foundation of China under Grant 51877182, and in part by the Science and Technology Projects of Sichuan Province under Grant 2018FZ0107. (*Corresponding author: Minwu Chen.*)

Y. Chen, M. Chen and Y. Liu are with the College of Electrical Engineering, Southwest Jiaotong University, Chengdu 611756, China (e-mail: yinyuchen@yahoo.com; chenminwu@home.swjtu.edu.com)

Z. Tian is with the Birmingham Centre for Railway Research and Education, School of Engineering, University of Birmingham, Birmingham B15 2TT, UK (e-mail: z.tian@bham.ac.uk).

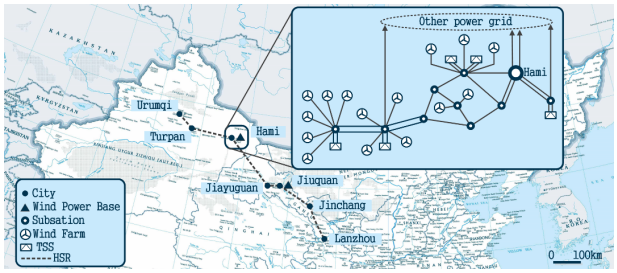

Fig. 1. Location of the Lanzhou-Urumqi HSR and partial power grid structure of Hami area

I. INTRODUCTION

VU PROBLEM caused by single-phase 25-kV AC TPSSs have attracted more and more attention in three-phase power grid, especially in northwest China [1]. Simultaneously, more than 32GW WPGs are installed in these remote areas due to the vast wind resource, which have reached the national total installed capacity of 17% in 2017 [2,3]. As shown in Fig. 1, Lanzhou-Urumqi HSR connects the northwest China, and passes through two super wind power bases (Hami and Jiuquan base). As the wind farm and TSS are generally connects to a PCC, according to the report [4], more than 67 pairs daily EMUs will be running on this line by 2025 and the rated power of an EMU is up to 20MW, the VU interrelationship between the TPSS and wind farm will more prominent. Therefore, implementing the VU management for TPSS is a significant method, which to regulate the system performance under the secure filed [5,6]. It involves two aspect: 1) carrying out the VU limit pre-assessment for unbalanced load, which ensured the VUF of PCC satisfy the requirements of national standard; 2) installing the VU compensation to make sure the VUF of unbalanced load meet the result of VU limit pre-assessment.

In regard of VU limit pre-assessment, IEC/TR 61000-3-13 guideline [7] provides a popular technical approach, there are some countries having adopted it to formulate themselves national standards, such as the Britain [8], Australia [9] and Denmark [10]. When implementing VU limit pre-assessment at

the PCC where connected large-scale wind farm, the attenuation influence of WPG on VU should be considered [11,12]. The unbalance load VU limit is depend on the apparent power ratio between the load and PCC, and a calculation method of apparent power of PCC has been proposed by IEC. Therefore, to address the problem, the attenuation impact of WPG can be quantified as power performance. The power performance of WPG under the unbalance condition have reported in [13], which injects positive-sequence power to grid, absorbs unbalance power at the same time. To reduce the power pulsations of WPG, the output power is described by sequence component voltage and current in [14,15]. Nevertheless, the drawback of modeling approach is cannot illustrate the VU impact on power performance of WPG directly, as well as the influence of VU angle is neglected that may arouse the calculation error [16,17].

Alternatively, there are a lot of technical schemes to improve the VUF of PCC. Some researchers have proposed various control schemes that adopt the wind farm for using as a VU compensator [18], However, there are two defects what ought to draw attention: 1) increasing the intensity of the train will deteriorate the VU condition at the PCC, leading to amount of wind farm capacity will use to compensation, and even interfere with the normal power output [19]; 2) the compensation performance is sharply constrained by the uncertainty of wind power. Therefore, compensating VU at the TSS is a reasonable technical scheme. In recent years, the railway power conditioner (RPC) technology and co-phase TPSS have been proposed to solve the power quality [20]-[23], unfortunately, RPC cannot eliminate the neutral section problem completely, which has aroused the serious accidents, Thus, take co-phase TPSS as an example in this paper. Obviously, the drawback is expensive cost compared with RPC, a partial compensating scheme have been presented in [22,23], which the compensation objective just satisfy the VU limit. In [23], a good VU control performance and a smaller compensation capacity are obtained by a novel calculation method for VU compensation order. However, due to the traditional calculation method of reference compensation current is inaccurate when massive WPGs are connected to an unbalanced PCC, causing the compensation result could unsatisfied [12]. Thus, building a novel mathematical model is necessary to portray the VU propagation behavior between the wind farm, TPSS and asymmetric grid. Furthermore, adopt the attenuation impact of WPG to optimize the compensation capacity.

This paper is organized as follows. A basic mathematical model of co-phase TPSS is introduced in section II. Section III analyzes the impact of DFIG connected with unbalanced power grid. The VU limit pre-assessment process in term of WPGs is discussed in Section IV. In Section V, A uniform VU propagation model is established; furthermore, a calculation method of reference compensation current is designed. Simulation result and case study respectively are given in Section VI and Section VII. Section VIII draws the conclusions.

II. Modelling of Co-phase TPSS

The co-phase TPSS structure is shown in Fig.2, a TT and a

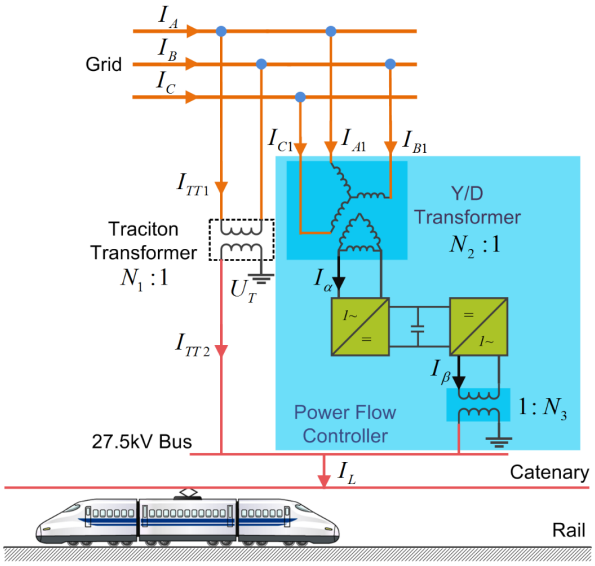

Fig. 2. Electrical configuration of co-phase TPSS

PFC work together to supply the power demand of the EMUs. As a result, the VU problem and low power factor can be fully or partly compensated by PFC. On the other hand, it could boost the availability of regenerative braking energy as the neutral section can be eliminated.

The current relationship between the various electrical ports can be expressed as:

$$\begin{bmatrix} \dot{I}_{\mathrm{A}} \\ \dot{I}_{\mathrm{B}} \\ \dot{I}_{\mathrm{C}} \end{bmatrix} = \begin{bmatrix} -\frac{1}{3N_2} & \frac{2}{3N_2} & -\frac{1}{3N_2} \\ \frac{1}{N_1} & 0 & -\frac{1}{N_1} \end{bmatrix}^{\mathrm{T}} \begin{bmatrix} \dot{I}_{TT2} \\ \dot{I}_{\alpha} \end{bmatrix} \tag{1}$$

where, $\dot{I}_{\mathrm{A}}$, $\dot{I}_{\mathrm{B}}$, $\dot{I}_{\mathrm{C}}$ is the three-phase current of power grid. $\dot{I}_{TT2}$ is the current in the traction side of the TT. $\dot{I}_{\alpha}$ is the current in the grid side (α side) of the PFC.

The voltage relationship between the various electrical ports can be expressed as:

$$\begin{bmatrix} \dot{U}_T \\ \dot{U}_{\alpha} \\ \dot{U}_{\beta} \end{bmatrix} = \begin{bmatrix} \frac{1}{N_1} & 0 & -\frac{1}{N_1} \\ -\frac{1}{3N_2} & \frac{2}{3N_2} & -\frac{1}{3N_2} \\ \frac{1}{N_1 N_3} & 0 & -\frac{1}{N_1 N_3} \end{bmatrix} \begin{bmatrix} \dot{U}_{\mathrm{A}} \\ \dot{U}_{\mathrm{B}} \\ \dot{U}_{\mathrm{C}} \end{bmatrix} \tag{2}$$

where,$\dot{U}_{\mathrm{A}}$, $\dot{U}_{\mathrm{B}}$, $\dot{U}_{\mathrm{C}}$ is the three-phase voltage of power grid. $\dot{U}_{\mathrm{T}}$ is the voltage in the traction side of the TT. $\dot{U}_{\alpha}$, $\dot{U}_{\beta}$is the voltage in the grid side (α side) and traction side (β side) of the PFC, respectively. N_1 is the ratio of the TT, N_2 is the ratio of the step-down transformer, N_3 is the ratio of the step-up transformer.

Furthermore, based on the (1) and (2), the sequence component of current and voltage aroused by the TPSS are given as follows:

$$\begin{bmatrix} \dot{T}^{+}_{TPSS} \\ \dot{T}^{-}_{TPSS} \end{bmatrix} = \begin{bmatrix} 1 & a & a^2 \\ 1 & a^2 & a \end{bmatrix} \begin{bmatrix} \dot{T}_{\mathrm{A}} & \dot{T}_{\mathrm{B}} & \dot{T}_{\mathrm{C}} \end{bmatrix}^{\mathrm{T}} \tag{3}$$

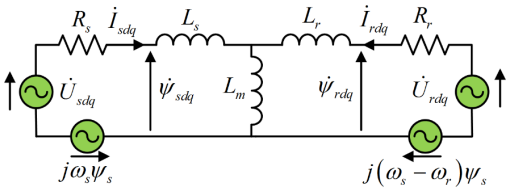

Fig. 3. Equivalent circuit of DFIG

where, a=$e^{j120°}$. The symbol "T" represents the three-phase current component or voltage component.

III. Analysis of DFIG System Connected with Unbalanced Power Grid

During the past decade, due to the excellent active and reactive power control capabilities, lower investment cost and power loss compared with the other WPG, the WPG based on the DFIG is widely installed in power grid in China [18].

A. Sequence component model of DFIG system

Under the positive synchronous (dq^+) reference frame rotating at angular speed rotor of ω_s, the DFIG equivalent circuit in stable state is shown in Fig. 3 [15].

According to the Fig.3, the stator and rotor flux $\dot{\psi}_{sdq}$ and $\dot{\psi}_{rdq}$ are given, respectively, by:

$$\dot{\psi}_{sdq} = L_s\dot{I}_{sqd} + L_m\dot{I}_{rqd} \tag{4}$$

$$\dot{\psi}_{rdq} = L_m\dot{I}_{sqd} + L_r\dot{I}_{rqd} \tag{5}$$

where, L_s and L_r are the self-inductances of stator and rotor winding, L_m is the mutual inductance, $\dot{I}_{sdq}$ and $\dot{I}_{rdq}$ are the current of stator and rotor winding.

According to (4) and (5), the rotor flux and stator current can be expressed as:

$$\dot{\psi}_{rdq} = \frac{L_m}{L_s}\cdot\dot{\psi}_{sdq} + \left(1-\frac{L_m^2}{L_rL_s}\right)L_r\dot{I}_{rdq} \tag{6}$$

$$\dot{I}_{sdq} = \frac{1}{L_s}\left(\dot{\psi}_{sdq} - L_m\dot{I}_{rdq}\right) \tag{7}$$

Further, the stator and rotor voltage $\dot{U}_{sdq}$ and $\dot{U}_{rdq}$ can be expressed as:

$$\dot{U}_{sdq} = R_s\dot{I}_{sdq} + j\omega_s\dot{\psi}_{sdq} \tag{8}$$

$$\dot{U}_{rdq} = R_r\dot{I}_{rdq} + j(\omega_s-\omega_r)\dot{\psi}_{rdq} \tag{9}$$

where, R_s and R_r are the resistance of stator and rotor winding, ω_s and ω_r is the angular frequency for stator and rotor.

Assuming no zero sequence components, the stator voltage and current can be decomposed into positive and negative sequence component under the unbalanced power grid, as shown in below:

$$\dot{U}_{sdq} = \dot{U}^+_{sdq} + \dot{U}^-_{sdq} \tag{10}$$

$$\dot{I}_{sdq} = \dot{I}^+_{sdq} + \dot{I}^-_{sdq} \tag{11}$$

Thus, the output power can be defined as three parts, which the part I, III is the positive power component S^+ and negative power component S^-, respectively, part II is the oscillation power S_{osc} that mainly induce the severe double frequency oscillation in DFIG system [15]. The part II and part III can be amalgamated into an unbalanced power component S_u based on the IEEE Std. 1459-2010.

$$S_{sdq} = \frac{3}{2}\dot{U}_{sdq}\dot{I}^*_{sdq} = \frac{3}{2}\left[\underbrace{\dot{U}^+_{sdq}\dot{I}^{+*}_{sdq}}_{\text{Part.I}} + \underbrace{\dot{U}^+_{sdq}\dot{I}^{-*}_{sdq} + \dot{U}^-_{sdq}\dot{I}^{+*}_{sdq}}_{\text{Part.II}} + \underbrace{\dot{U}^-_{sdq}\dot{I}^{-*}_{sdq}}_{\text{Part.III}}\right] \tag{12}$$

According to Fig. 3, the electromagnetic torque is equal to the sum of the power outputs from the $j\omega_s\psi_s$ and $j(\omega_s-\omega_r)\psi_r$, and then multiply by $1/\omega_r$. Therefore, associating with (6), (7) and (8), and neglect the voltage drop on the stator resistance, the electromagnetic torque is expressed as:

$$\begin{aligned} T_e &= -\frac{3}{2}\Re\left\{j\omega_s\dot{\psi}_{sdq}\dot{I}^*_{sdq} + j(\omega_s-\omega_r)\psi_{rdq}\dot{I}^*_{rdq}\right\} \\ &= -\frac{3}{2}\left[\omega_sL_m\left(I_{rd}I_{sq}-I_{rq}I_{sd}\right)+(\omega_s-\omega_r)L_m\left(I_{rd}I_{sq}-I_{rq}I_{sd}\right)\right] \\ &= -\frac{3}{2}\left[\frac{L_m}{L_s}\Im\left\{\left(L_s\dot{I}_{sqd}+L_m\dot{I}_{rqd}\right)\dot{I}^*_{rdq}\right\}\right] = -\frac{3}{2}\frac{L_m}{L_s}\Re\left\{j\dot{\psi}_{sdq}\dot{I}^*_{rdq}\right\} \\ &= \frac{3}{2}\Im\left\{\dot{\psi}_{sdq}\dot{I}^*_{sdq}\right\} = -\frac{3}{2}\frac{1}{\omega_s}\Re\left\{\dot{U}_{sdq}\dot{I}^*_{sdq}\right\} \end{aligned} \tag{13}$$

B. Quantifying the impact of VU on DFIG system

The definition of VUF is widely adopted to quantify the VU in some national standard or recommendations, such as the IEC 61000-4-30, IEEE1159-1995. The VUF is defined as:

$$\text{VUF} = \left|\frac{\dot{U}^-_{sdq}}{\dot{U}^+_{sdq}}\right|\times 100\% \tag{14}$$

However, there are some recent studies debating its effectivity [16,17]. Some researchers propose that (14) is not adequately reliable to quantify the input power, electromagnetic torque, power factor and *etc.* There are two main reason should be pointed out. Firstly, the difference angle between the negative sequence component and positive sequence component is also a distinct variable; and secondly, there are so many VU combinations under the same value of this index.

Therefore, a new definition that called the complex voltage unbalance factor (CUVF) is proposed to overcome above insufficiency. It can be expressed as:

$$\text{CVUF} = \frac{\dot{U}^-_{sdq}}{\dot{U}^+_{sdq}}\times 100\% \tag{15}$$

Furthermore, the complex current unbalance factor is defined as:

$$\text{CCUF} = \frac{\dot{I}^-_{sdq}}{\dot{I}^+_{sdq}}\times 100\% \tag{16}$$

Specially, the relationship between the CVUF and CCUF in DFIG system can be expressed as [16]:

$$\text{CCUF} = \frac{Z^+_{sdq}}{Z^-_{sdq}}\times \text{CVUF} \tag{17}$$

Based on above mathematical definition, the output power of DFIG can be rewritten as:

$$\begin{aligned} S_{sdq} &= \frac{3}{2}\left(\dot{U}^{+}_{sdq}\dot{I}^{+*}_{sdq} + \dot{U}^{+}_{sdq}\dot{I}^{-*}_{sdq} + \dot{U}^{-}_{sdq}\dot{I}^{+*}_{sdq} + \dot{U}^{-}_{sdq}\dot{I}^{-*}_{sdq}\right) \\ &= \frac{3}{2}\dot{U}^{+}_{sdq}\dot{I}^{+*}_{sdq} \times \left[1 + \frac{Z^{+}_{sdq}}{Z^{-}_{sdq}}\left(\mathrm{CVUF}^{*} + \left|\mathrm{CVUF}\right|^{2}\right) + \mathrm{CVUF}\right] \\ &= S^{+} + S^{+} \times \left[\frac{Z^{+}_{sdq}}{Z^{-}_{sdq}}\left(\mathrm{CVUF}^{*} + \left|\mathrm{CVUF}\right|^{2}\right) + \mathrm{CVUF}\right] \\ &= S^{+} + S_{u} \end{aligned} \tag{18}$$

The electromagnetic torque of DFIG can be rewritten as:

$$\begin{aligned} T_e &= -\frac{3}{2}\frac{1}{\omega_s}\Re\left\{\dot{U}_{sdq}\dot{I}^{*}_{sdq}\right\} \\ &= -\frac{1}{\omega_s}P^{+} \times \Re\left\{1 + \frac{Z^{+}_{sdq}}{Z^{-}_{sdq}}\left(\mathrm{CVUF}^{*} + \left|\mathrm{CVUF}\right|^{2}\right) + \mathrm{CVUF}\right\} \\ &= T_{ste} + T_{osc} \end{aligned} \tag{19}$$

Thus, according to the (18) and (19), the mapping between the VU index and the key electrical parameters of wind power generator is established.

IV. VU Limit Pre-assessment Process in Terms of DFIG-based Wind Farm

A. VU Limit Allocation Method in IEC/TR 61000-3-13

To fairly regulate the system VU level and allocate the VU limit of an unbalanced load, IEC/TR 61000-3-13 follows the three-stage pre-assessment process:

- Stage 1: If the ratio of the power equivalent of customer *j* and the grid short-circuit capacity of bus *x* satisfies (20), customer *j* can directly connect to the public grid.

$$\frac{S_{x:j}}{S_{dc:x}} \le 0.2\% \tag{20}$$

where $S_{dc:x}$ is the short-circuit capacity of bus *x*, and $S_{x:j}$ is the apparent power of customer installation *j* at bus *x*, which can be defined as:

$$\begin{aligned} S_{x:j} &= \sqrt{\left(U^{+}I^{+}\right)^{2} + \left(U^{-}I^{+} + U^{+}I^{-} + U^{-}I^{-}\right)^{2}} \\ &= \sqrt{S^{2}_{p\_x:j} + S^{2}_{u\_x:j}} \end{aligned} \tag{21}$$

where, $S_{p\_x:j}$ and $S_{u\_x:j}$ are positive power and unbalance power of customer installation *j* at bus *x*, respectively.

- Stage 2: If customer *j* is hard to meet the requirement of stage 1, it should comply with a VU limit ($E_{x:j}$). The VU limit pre-assessment method is expressed as:

$$E_{x:j} = \sqrt[\alpha]{Kue_x}\,U_{g:x}\sqrt[\alpha]{\frac{S_{x:j}}{S_{tot:x}}} \tag{22}$$

where $U_{g:x}$ is the bus planning level, Kue_x represents the fraction of $U_{g:x}$ that can be allocated to customer installations, when the transmission line is symmetrical, and Kue_x=1. α is an exponent, the indicative value is 1.4. $S_{tot:x}$ is the total available

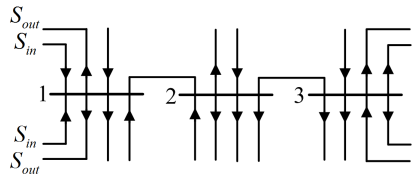

Fig. 4. Determination of S_i

apparent power of the entire system that considers the VU contributions from adjacent busbars 1, 2, …, *n* in terms of influence coefficients $k_{i:x}$:

$$S_{tot:x} = k^{\alpha}_{1:x}S_1 + k^{\alpha}_{2:x}S_2 + \ldots + S_x + \ldots + k^{\alpha}_{n:x}S_n \tag{23}$$

Unfortunately, there is a notable defect that the result of equation (22) renders the actual bus VU level higher than the planning level, even when no VUF of a customer exceeds the VU limit [24]. Thus, an improved method is developed to strictly regulate the VU level of bus, which is called the constraint bus voltage method:

$$E_{x:j} = k_a \sqrt[\alpha]{Kue_x S_{x:j}} \tag{24}$$

where k_a is the allocated coefficient, which can be expressed as:

$$k_a = \frac{U_{g:x}}{\max\left[\sqrt[\alpha]{S_x + \sum_{i=1}^{n}\left(k^{\alpha}_{i:x}S_i\right)}\right]} \tag{25}$$

- Stage 3: If customer *j* cannot meet the requirement of stage 2, the customer should consult the operator of the public grid.

B. Allocation Principle for VU Attenuation Ability of DFIG-based Wind Farm

As shown in Fig. 4, according to the power definition in IEC/TR 61000-3-13, the value of S_i is calculated based on (26). S_{out} is defined as the power flow leaving from the bus.

$$S_i = \sum S_{out} \quad (i \in 1,2,\ldots,x,\ldots,n) \tag{26}$$

When WPGs are connected to an unbalance power grid, they absorb unbalanced power and inject positive power to power grid [13]. It means that the unbalance power is consumed by WPGs, and the VUF is reduced compared with un-connected WPGs.

Therefore, according to the IEC/TR 61000-3-13, the unbalance power is regard as S_{out}, (26) can be rewritten as:

$$S_i = S_{u:WF} + \sum S_{out} \quad (i \in 1,2,\ldots,x,\ldots,n) \tag{27}$$

Obviously, calculating unbalance power should be strictly complied with the national standard to achieve the operation performance of wind farm under the secure filed. According to the requirement of technical guideline for connecting wind farm to power system, such as GB/T 19963-2011 in China: wind farm should work well when the VUF at PCC less than 2%. Therefore, when applying the VU limit pre-assessment, the value of unbalance power for wind farm take the highest as S_{out} when VUF is equal to 2%.

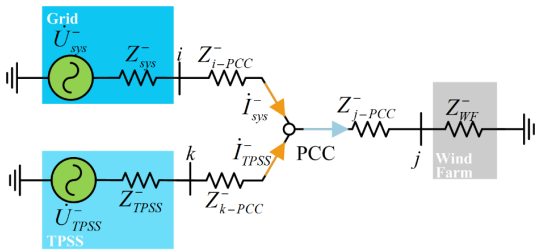

Fig. 5. Negative sequence equivalent circuit of power system.

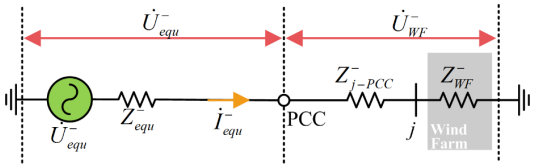

Fig. 6. Asymmetric source simplified circuit

In order to examine the validity of improved allocated method, IEC proposed a general summation law [24].

$$\mathrm{VUF}_{x:j}=\sqrt[\alpha]{\left(k_{1:x}E_{1:}\right)^{\alpha}+\left(k_{2:x}E_{2}\right)^{\alpha}+\ldots+\left(E_{x}\right)^{\alpha}+\ldots+\left(k_{n:x}E_{n}\right)^{\alpha}} \quad (28)$$

V. VU Compensation Approach for TPSS

The traditional calculation approach of reference VU compensation current has been adopted in various works [21]-[23]:

$$\mathrm{VUF}_{x:j}=\frac{S_{u\_x:j}}{S_{dc:x}}\cdot\mathrm{CUF}_{x:j} \quad (29)$$

However, there is an assumption that VUF at bus x cannot interfere the CUF of customer installation j, which means this assumption is invalid when the bus x supplies large proportions of WPGs, due to a small VU will arouse a huge imbalance current at WPG [12]. Therefore, to address above obstacle, there is an urgent demand to establish a novel mathematical relationship between the $\mathrm{VUF}_{x:j}$ and $\mathrm{CUF}_{x:j}$ in this scenario.

A. Uniform VU Propagation Model

Considering the TPSS, wind farm and equivalent unbalance grid as shown in Fig. 5. The three bus i, j and k respectively are connected to the PCC bus. The purpose is to assess the VUF at the PCC which is aroused by the single-phase TPSS at the k bus and the equivalent unbalance grid at the i bus.

1) The CVUF at the PCC

Referring to Fig. 5, two asymmetric voltage sources ($\dot{U}^-_{sys}$, $\dot{U}^-_{TPSS}$) can be equal to an equivalent asymmetric voltage source $\dot{U}^-_{equ}$, as shown in Fig. 6, and detailed derivations given in *Appendix A*.

The negative sequence voltage at the PCC can be expressed as:

$$\dot{U}^-_{PCC}=\frac{Z^-_{WF}+Z^-_{j-PCC}}{Z^-_{equ}+Z^-_{WF}+Z^-_{j-PCC}}\dot{U}^-_{equ} \quad (30)$$

where, Z^-_{j-PCC} is the negative sequence impedance of transmission line, Z^-_{WF} and Z^-_{equ} respectively are the negative sequence impedance of wind farm and equivalent asymmetric voltage source.

Furthermore, the equivalent asymmetric voltage source $\dot{U}^-_{equ}$ can be given by (31):

$$\dot{U}^-_{equ}=\dot{I}^-_{equ}Z^-_{equ}=\mathrm{CCUF}_{equ}\frac{\dot{U}^+_{equ}}{Z^+_{equ}}\cdot Z^-_{equ} \quad (31)$$

where, Z^+_{equ} is the positive impedance of equivalent asymmetric voltage source.

CVUF at the PCC bus (CVUF_{PCC}) can be expressed as:

$$\mathrm{CVUF}_{PCC}=\frac{Z^-_{WF}+Z^-_{j-PCC}}{Z^-_{equ}+Z^-_{WF}+Z^-_{j-PCC}}\frac{\dot{U}^+_{equ}}{\dot{U}^+_{PCC}}\frac{Z^-_{equ}}{Z^+_{equ}}\cdot\mathrm{CCUF}_{equ} \quad (32)$$

According to the reference [25], the term $\dot{U}^+_{equ}/\dot{U}^+_{PCC}$ in (32) can be re-written in terms of the positive sequence impedance:

$$\frac{\dot{U}^+_{equ}}{\dot{U}^+_{PCC}}=1+\frac{Z^+_{equ}}{Z^+_{WF}+Z^+_{j-PCC}} \quad (33)$$

At the same time, CCUF relationship between the equivalent asymmetric voltage source and TPSS can be given as:

$$\mathrm{CCUF}_{equ}=\frac{\dot{I}^-_{equ}}{\dot{I}^+_{equ}}=\frac{Z^-_{i-PCC}+Z^-_{k-PCC}}{Z^+_{i-PCC}+Z^+_{k-PCC}}\frac{Z^+_{i-PCC}}{Z^-_{i-PCC}}\frac{\dot{I}^-_{TPSS}}{\dot{I}^+_{TPSS}} \quad (34)$$

Therefore, CVUF at the PCC bus (CVUF_{PCC}) can be re-written as:

$$\mathrm{CVUF}_{PCC}=c_1\cdot c_2\cdot c_3\cdot c_4\cdot\mathrm{CCUF}_{TPSS} \quad (35)$$

where,

$$\begin{cases} c_1=\dfrac{Z^-_{WF}+Z^-_{j-PCC}}{Z^-_{equ}+Z^-_{WF}+Z^-_{j-PCC}},\quad c_2=1+\dfrac{Z^+_{equ}}{Z^+_{WF}+Z^+_{j-PCC}} \\ c_3=\dfrac{Z^-_{equ}}{Z^+_{equ}},\quad c_4=\dfrac{Z^-_{i-PCC}+Z^-_{k-PCC}}{Z^+_{i-PCC}+Z^+_{k-PCC}}\dfrac{Z^+_{i-PCC}}{Z^-_{i-PCC}} \end{cases} \quad (36)$$

2) The CVUF at the k bus

According to Fig. 5, the positive sequence voltage and negative sequence voltage at the PCC bus can be given in (37) and (38):

$$\dot{U}^+_{PCC}=\dot{U}^+_{TPSS}+\dot{I}^+_{TPSS}\left(Z^+_{k-PCC}+Z^+_{TPSS}\right) \quad (37)$$

$$\dot{U}^-_{PCC}=\dot{U}^-_{TPSS}-\dot{I}^-_{TPSS}\left(Z^-_{k-PCC}+Z^-_{TPSS}\right) \quad (38)$$

CVUF at the k bus (CVUF_{TPSS}) can be obtained by (37):

$$\mathrm{CVUF}_{TPSS}=\frac{U^+_{PCC}}{U^+_{TPSS}}\cdot\mathrm{CVUF}_{PCC}+\frac{Z^-_{k-PCC}+Z^-_{TPSS}}{Z^+_{k-PCC}+Z^+_{TPSS}}\cdot\mathrm{CCUF}_{TPSS} \quad (39)$$

Similarly, the term $\dot{U}^+_{PCC}/\dot{U}^+_{TPSS}$ in (39) can be re-written in terms of the positive sequence impedance (see *Appendix A*). Therefore, CVUF at the k bus (CVUF_{TPSS}) can be re-written as:

$$\mathrm{CVUF}_{TPSS}=k_1\cdot\mathrm{CVUF}_{PCC}+k_2\cdot\mathrm{CCUF}_{TPSS} \quad (40)$$

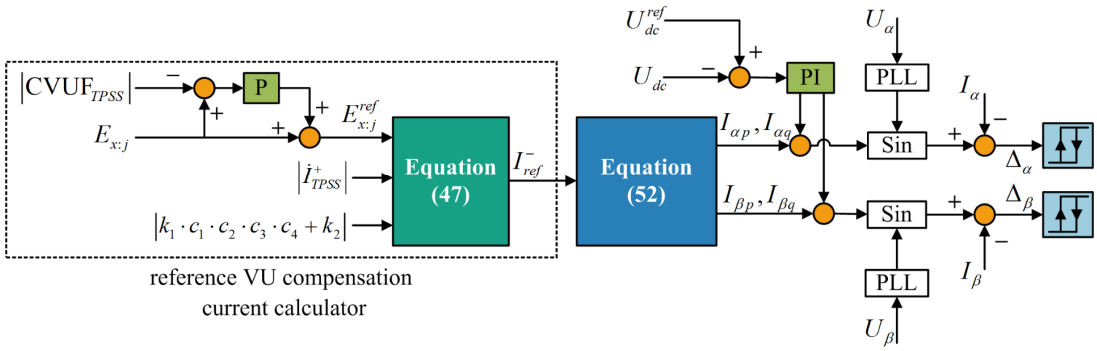

Fig. 7. Schematic diagram of proposed compensation strategy

where

$$k_1 = 1 - \frac{Z^+_{k-PCC} + Z^+_{TPSS}}{Z^+_{TPSS}}, k_2 = \frac{Z^-_{k-PCC} + Z^-_{TPSS}}{Z^+_{k-PCC} + Z^+_{TPSS}} \tag{41}$$

On the other words, CVUF at the k bus (CVUF_{TPSS}) is not only impact by TPSS, but also influenced by unbalance power grid.

3) The CVUF at the j bus

According to Fig. 6, the positive sequence voltage and negative sequence voltage at the PCC bus can be given in (42) and (43):

$$\dot{U}^+_{PCC} = \dot{U}^+_j - \dot{I}^+_{wf} Z^+_{j-PCC} \tag{42}$$

$$\dot{U}^-_{PCC} = \dot{U}^-_j + \dot{I}^-_{wf} Z^-_{j-PCC} \tag{43}$$

The CVUF at the j bus (CVUF_{WF}) can be expressed as (44):

$$\mathrm{CVUF}_{WF} = \frac{\dot{U}^+_{PCC}}{\dot{U}^+_j} \cdot \mathrm{CVUF}_{PCC} - \frac{\dot{I}^+_{wf} Z^-_{j-PCC}}{\dot{U}^+_j} \cdot \mathrm{CCUF}_{WF} \tag{44}$$

In the same way, $\dot{U}^+_{PCC}/\dot{U}^+_j$ in (43) can be re-written in terms of the positive sequence impedance. Therefore, CVUF at the j bus (CVUF_{TPSS}) can be re-written as:

$$\mathrm{CVUF}_{WF} = m_1 \cdot \mathrm{CVUF}_{PCC} - m_2 \cdot \mathrm{CCUF}_{WF} \tag{45}$$

where,

$$m_1 = 1 + \frac{Z^+_{j-PCC}}{Z^+_{WF}}, m_2 = \frac{Z^-_{j-PCC}}{Z^+_{WF}} \tag{46}$$

B. Proposed Compensation Strategy of Co-phase TPSS

Based on the proposed uniform VU propagation model and [23], a novel compensation strategy is proposed via associating with (25), (33) and (38), as shown in Fig. 7. On the other hand, in order to improve the tracking performance of compensation strategy, a proportional controller is introduced to the VUF reference current calculator. The proportional control of error can be expressed as:

$$E^{ref}_{x:j} = K_p \left(E_{x:j} - \left| \mathrm{CVUF}_{TPSS} \right| \right) + E_{x:j} \tag{47}$$

where, K_p is proportional gain.

Thus, the VUF reference current can be expressed as:

$$I^-_{ref} = \frac{\left| \dot{I}^+_{TPSS} \right|}{\left| k_1 \cdot c_1 \cdot c_2 \cdot c_3 \cdot c_4 + k_2 \right|} E^{ref}_{x:j} \tag{48}$$

According to the p-q transformer theory, taking each voltage as a reference, the currents $\dot{I}_{TT}$, $\dot{I}_\alpha$, $\dot{I}_\beta$, $\dot{I}_L$ can be divided to a p-axis component and a q-axis component, respectively.

$$\begin{cases} \dot{I}_{TT2} = I_{TTp} + jI_{TTq} \\ \dot{I}_\alpha = I_{\alpha p} + jI_{\alpha q} \\ \dot{I}_\beta = I_{\beta p} + jI_{\beta q} \\ \dot{I}_L = I_{Lp} + jI_{Lq} \end{cases} \tag{49}$$

Associating with (1) and (3), the traction side current I_{TTp}, I_{TTq} can be expressed as [23]:

$$\begin{cases} I_{TTp} = \dfrac{2\sqrt{3}N_1 x_1 - 6N_1 x_2 + I_{Lp} + 3I_{Lp}}{8} \\ I_{TTq} = \dfrac{6N_1 x_1 + 2\sqrt{3}N_1 x_2 + 3I_{Lp} - I_{Lp}}{8} \end{cases} \tag{50}$$

where,

$$x_1 = -I^-_{ref} \cos\left(-60^\circ + \varphi_L\right),\ x_2 = -I^-_{ref} \sin\left(-60^\circ + \varphi_L\right) \tag{51}$$

Furthermore, the PFC compensation current for grid side (α side) and traction side (β side) can be expressed as:

$$\begin{cases} I_{\alpha p} = \dfrac{\sqrt{3}N_2}{N_1}\left(I_{Lp} - I_{TTp}\right) \\ I_{\alpha q} = -\dfrac{\sqrt{3}N_2}{N_1} I_{TTq} \\ I_{\beta p} = N_3\left(I_{Lp} - I_{TTp}\right) \\ I_{\beta q} = N_3\left(I_{Lq} - I_{TTq}\right) \end{cases} \tag{52}$$

VI. Simulation Results

In this section, an IEEE-9 bus test system is introduced to testify the VU limit pre-assessment process and compensation strategy, as shown in Fig. 8. The parameters of test system are given in *Appendix B*. A TSS is connected to 11th bus, and a 150MVA wind farm is attached to 10th bus, 5th bus is PCC, all the customers are connected to the asymmetric grid, source-3 is

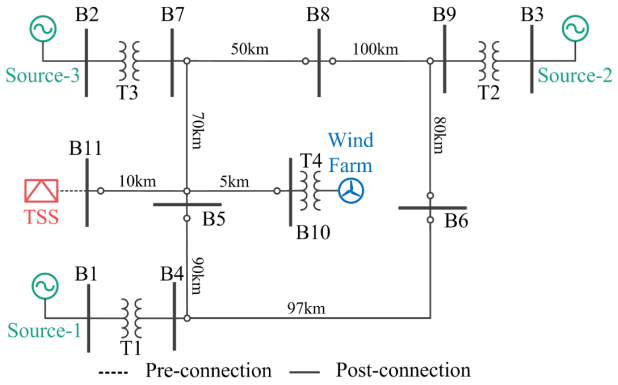

Fig. 8. IEEE 9-bus test system

TABLE I
PARAMETERS OF PFC FOR TPSS

Parameters	Values
α phase voltage U_α	10kV
α phase inductor L_α	20mH
β phase voltage U_β	2kV
β phase inductor L_β	3mH
DC-link voltage U_{dc}	3kV
DC capacitor C_{dc}	40mF
Ratio of transformer N_1	8
Ratio of transformer N_2	12.7
Ratio of transformer N_3	14

TABLE II
PARAMETERS OF THE 1.5 MVA DFIG SYSTEM

Parameters	Values
Stator voltage U_s	575V
Paris of poles	3
Reference voltage U_{base}	330V
Reference current I_{base}	1506A
Stator resistance R_s	0.023
Stator inductance L_s	0.18
Rotor resistance R_r	0.016
Rotor inductance L_r	0.16
Field inductance L_m	2.9
DC-link voltage U_{dc}	1150V
DC capacitor C_{dc}	10μF

TABLE III
PARAMETERS OF THE 1.5 MW DFIG SYSTEM

	Case 1	Case 2	Case 3
Traction Load S_L	15MVA	30MVA	30MVA
PF of EMUs	0.95	0.95	0.95
Target $E_{x:j}^{ref}$	2%	2%	4%
Time interval	0s~3s	3s~4s	4s~5s

TABLE IV
COMPARISONS BETWEEN IMPROVED STRATEGY AND PROPOSED STRATEGY IN [23]

	Case 2 in [23]	Case 2 in this paper
S_L (MVA)	30	30
$E_{x:j}^{ref}$ (%)	2%	2%
U_α, U_β (kV)	27.5	27.5
I_α (A)	275	189
I_β (A)	194	176
S_{PFC} (MVA)	12.89	10.04
ΔS_{PFC} (pu)	0%	-22%

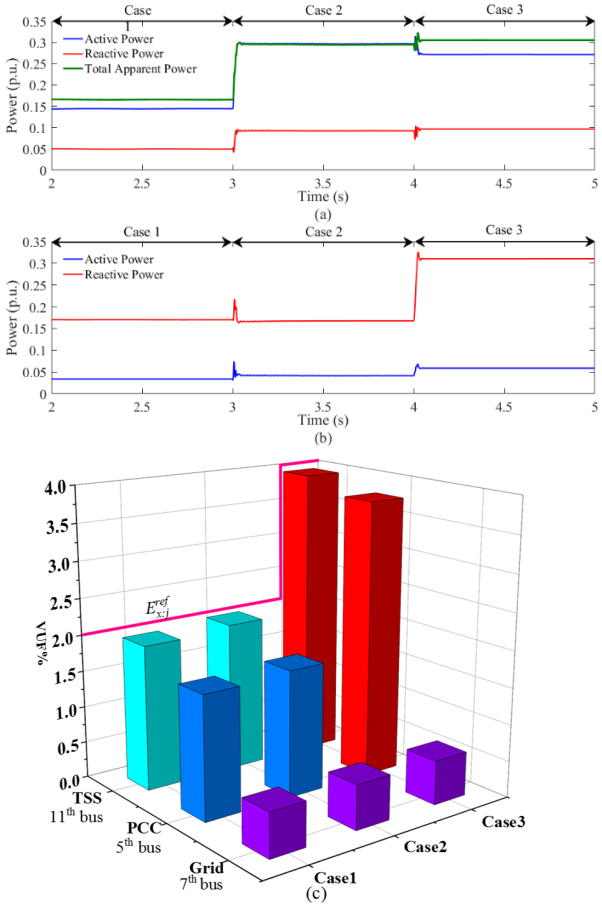

Fig. 9. Simulation result of power consumption and VUF performance. (a) positive-sequence power and total apparent power of TSS, (b) unbalance power of TSS, (c) VUF performance

unbalance source. The parameters of DFIG and PFC of novel TPSS are respectively shown in Table I. and Table II.

A. Verification of Proposed Compensation Strategy

In order to better verify the performance of proposed compensation strategy, three cases are considered, as shown in Table III. Before 3.00s, the compensation target is set to 2% according to the requirement of national standard, the traction load is equal to 15MVA, which can performance the load characteristic of EMUs applied to high-speed railway. In order to simulate the impact characteristic of EMUs, the traction load changes from 15 to 30MVA at 3.00s. The VU compensation commend is increase from 2% to 4% at 4.00s, which to demonstrate the trace ability of proposed compensation strategy.

Fig. 9 shows the simulation result of power consumption and VUF performance. It can be seen that, the VUF of grid is set as 0.6%, the unbalance power in Fig. 9(b) and VUF of TSS in Fig. 9(c) are stable when positive-sequence power in Fig. 9(a) increases from 15 to 30MVA; on the other hand, the VUF of TSS well matches with $E_{x:j}^{ref}$ when VU compensation target changes from 2% to 4% in Fig. 9(c). The results reveal the validity of proposed uniform VU propagation model and VU compensation approach.

The comparison between improved strategy in this paper and the strategy proposed in [23] is shown in Table IV. It is

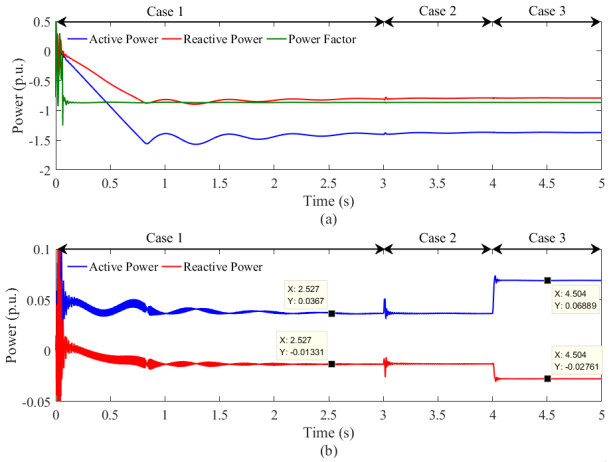

Fig. 10. Simulation result of power flow of DFIG-based wind farm at 10th bus. (a) positive-sequence power and power factor, (b) unbalance power

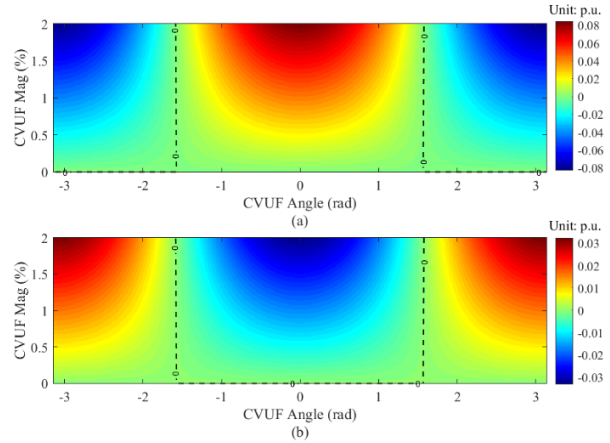

Fig. 11. The VU impact on DFIG-based wind farm. (a) unbalanced active power, (b) unbalanced reactive power

prominent to see that the capacity of PFC is decreased by 22% to 10.04MVA. Thus, it can be concluded that the proposed calculation method of reference VU compensation current is available.

B. Analysis the VU Impact on Wind Farm

Fig. 10 shows the simulation result of power flow of windfarm. The wind farm is absorbing unbalanced active power, injecting positive-sequence power and unbalanced reactive power to power grid when it connected to the unbalance power grid, this phenomenon is consistent with the conclusion in Section IV-B.

Table IV. shows the comparison of unbalance power using equation (18) and simulation result. CVUF values come from Fig. 9. It can be seen that, the error of unbalanced apparent power between the formula calculation and simulation result less than 5%. The discrepancy arises as the idealization made in origin of (18). Thus, the error is accepted, which means (18) can apply to quickly estimate the VU impact on DFIG-based wind farm.

Fig. 11 illustrates the VU impact on DFIG-based wind farm using (18). On the one hand, not only the magnitude of CVUF but also the angle of CVUF can significantly affect the unbalance power. On the other hand, according to the Fig. 12,

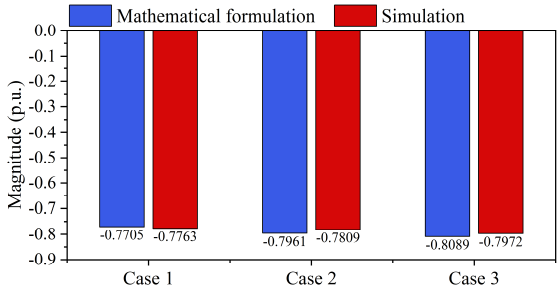

Fig. 12. Comparison of electromagnetic torque using mathematical formulation and simulation

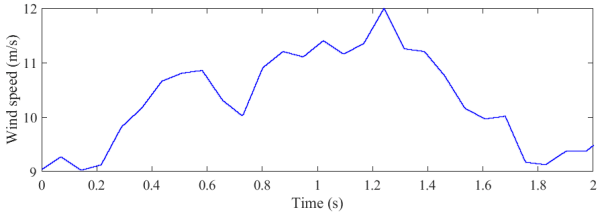

Fig. 13. Time-varying wind speed

TABLE V
COMPARISON OF UNBALANCE POWER

		Values	
CVUF at 10th bus		0.978∠-0.051	1.978∠-0.059
Active power	Equation (18)	0.0376	0.0670
	Simulation	0.0367	0.0689
Reactive power	Equation (18)	-0.0144	-0.0230
	Simulation	-0.0135	-0.0276
Apparent power	Equation (18)	0.0402	0.0708
	Simulation	0.0391	0.0742
	Error	+2.81%	-4.5%

the grid operator can available the performance of wind farm. When the capacity of wind farm is equal to 150MVA (1.5 p.u.), the wind farm will absorb 8.5MVA unbalance power under the secure filed border at most. According to the discussion in Section IV-B, this part power can deem as performance of VU attenuation ability.

Fig. 12 exhibits the comparison result of electromagnetic torque using mathematical formulation and simulation. The calculation results derived from (19) shows a minor discrepancy compared with simulation, on the other word, (19) can be used to portray the VU impact on electromagnetic torque under the steady state.

C. Sensitive Analysis

Actually, WPG is variable in nature as the variability of wind speed, the wind speed between 9-12 m/s is considered to verify the stability of proposed model, as shown in Fig. 13.

Fig. 15 shows the simulation result of CVUF of TSS, under the proposed VU compensation strategy, the magnitude of CVUF of TSS is fluctuating at 2%, which demonstrates the efficiency of the proposed VU compensation strategy.

As a result, the power demand of TSS is shown in Fig. 16. EMUs are frequently drawing or regeneration braking due to the complex mountainous terrain in western China, and the instantaneous power has arrived 48.56MVA (0.4856 p.u.).

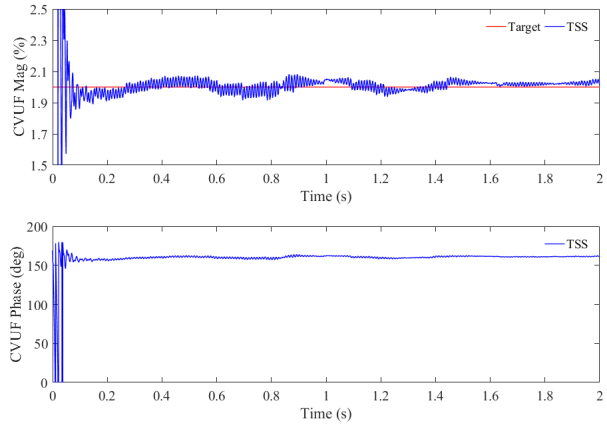

Fig. 14. Simulation result of CVUF of TSS

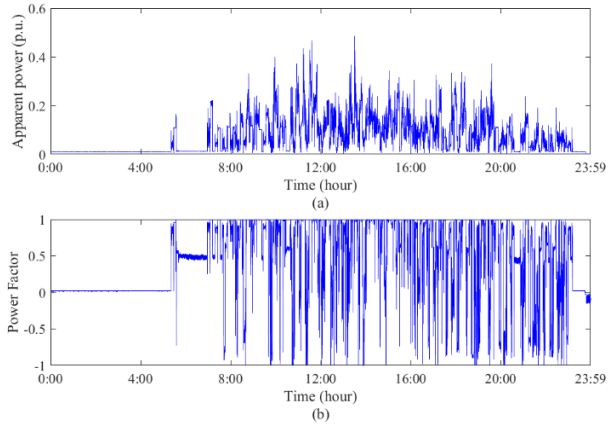

Fig. 15. Power demands of TSS during 24h. (a) total apparent power of TSS, (b) power factor of TSS

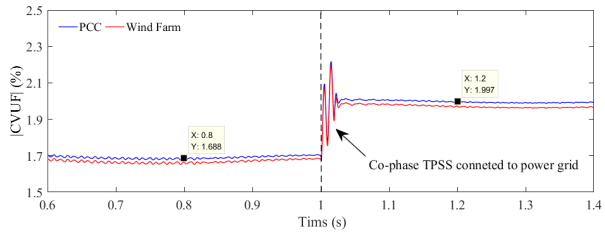

Fig. 16. Verification of VU limit pre-assessment result

TABLE VI
VU LIMIT PRE-ASSESSMENT RESULT

Bus Num.		$S_{x:j}$ (MVA)	$S_{tot:x}$ (MVA)	k_a	$E_{x:j}$ (%)
4th	Bus load	0	164.72		
5th	Bus load	71.92	113.27		
	Traction Load	32.85			0.4082
	Wind farm	8.5		0.0185	
6th	Bus load	94.86	94.86		
7th	Bus load	0	172.49		
8th	Bus load	105.95	105.94		
9th	Bus load	0	157.10		

D. VU limit pre-assessment

The bus load $S_{x:j}$, total available apparent power $S_{tot:x}$, influence coefficients k_a and VU limit of TPSS $E_{x:j}$ are listed in Table VI. The DFIG-based wind farm will support 8.5MVA to participate in VU limit pre-assessment process based on the conclusion in Section VI-B. Based on the filed test, the apparent power of TSS is 32.85MVA. As a result, the VU limit of TSS is 0.4082%.

E. Verification of pre-assessment result

According to the principle of IEC/TR 61000-3-13, the VUF at PCC shall not exceed 2% when all the unbalanced customer emission allocated VU limit. Thus, when actual VUF of TSS is equal to 0.4082%, the 1.688% is tolerated by power grid, based on the general summation law in (28). The simulation result is shown in Fig. 18, the TSS connected to asymmetric power grid at 1.0s, the simulation result is consistent with above conclusion; on the other hand, actual VUF of wind farm less than 2%, which satisfied the requirement of GB/T 19963-2011 in China. Therefore, the effective of developed VU limit pre-assessment is demonstrated by simulation result.

VII. CONCLUSION

In this paper, an VU management approach for HSR is proposed, which includes an VU limit pre-assessment process in terms of the influence of wind farm, and a novel VU compensation strategy of TPSS.

The mapping between the CVUF and the key electrical parameters of WPG is established, which reveals the effect of magnificent and angle of VU on output power and electromagnetic torque. Furthermore, according to the definition of IEC/TR 61000-6-13, the unbalanced power of wind farm can regard as apparent power of bus, the VU limit pre-assessment considered the impact of wind farm is accomplished. On the other hand, to portray the VU propagation behavior between the TPSS, wind farm and asymmetric grid, a uniform mathematical model is built. Based on this model, a novel calculation approach of reference compensation current is presented to provide an accurate command to TPSS. The correctness of the improved VU limit pre-assessment process and the validity of VU compensation of TPSS are demonstrated by an IEEE-9 bus test system.

At present, China government is establishing a new railway from Sichuan to Tibet using 10 years. Due to the extremely weak power grid, more than two TSSs will connect to a substation. Nevertheless, the vast renewable resource cannot neglect. Thus, in order to reduce the cost and fully utilize renewable resource, how to coordinate reference compensation current between the different TSSs is worth discussing in the future.

APPENDIX A
SEQUENCE COMPONENT CALCULATION

The positive sequence impedance of equivalent asymmetric voltage source Z^{+}_{equ} can be expressed as:

$$Z^{+}_{equ}=\frac{\left(Z^{+}_{sys}+Z^{+}_{i-PCC}\right)\left(Z^{+}_{TPSS}+Z^{+}_{k-PCC}\right)}{\left(Z^{+}_{sys}+Z^{+}_{i-PCC}\right)+\left(Z^{+}_{TPSS}+Z^{+}_{k-PCC}\right)} \tag{A1}$$

The negative sequence impedance of equivalent asymmetric voltage source Z^{-}_{equ} can be expressed as:

$$Z_{equ}^{-}=\frac{\left(Z_{sys}^{-}+Z_{i-PCC}^{-}\right)\left(Z_{TPSS}^{-}+Z_{k-PCC}^{-}\right)}{\left(Z_{sys}^{-}+Z_{i-PCC}^{-}\right)+\left(Z_{TPSS}^{-}+Z_{k-PCC}^{-}\right)} \tag{A2}$$

The positive sequence impedance of wind farm Z_{WF}^{+} can be expressed as:

$$Z_{WF}^{+}=\frac{\left(\frac{R_s}{s}+j2\pi fL_r\right)\cdot j2\pi fL_m}{\frac{R_s}{s}+j2\pi fL_r+j2\pi fL_m}+R_s+j2\pi fL_s \tag{A3}$$

The negative sequence impedance of wind farm Z_{WF}^{-} can be expressed as:

$$Z_{WF}^{-}=\frac{\left(\frac{R_s}{2-s}+j2\pi fL_r\right)\cdot j2\pi fL_m}{\frac{R_s}{2-s}+j2\pi fL_r+j2\pi fL_m}+R_s+j2\pi fL_s \tag{A4}$$

APPENDIX B
PARAMETERS OF IEEE-9 BUS TEST SYSTEM

The transformer parameters are shown in Table IX.

TABLE VII
TRANSFORMER PARAMETERS

	T1	T2	T3	T4
Rated primary voltage (kV)	24	18	15.5	0.575
Rated secondary voltage (kV)	230	230	230	230
R_1 (p.u.)	0.1	0.1	0.1	0.1
X_1 (p.u.)	0.0288	0.0313	0.0293	0.515
R_2 (p.u.)	0.1	0.1	0.1	0.1
X_2 (p.u.)	0.0288	0.0313	0.0293	0.515
R_m (p.u.)	500	500	500	500
X_m (p.u.)	800	800	800	800

The impedance matrix of the transposed line (Ω/km):

$$\begin{pmatrix} 0.2952+j0.7423 & 0.04622+j0.2882 & 0.04620+j0.2448 \\ 0.04622+j0.2882 & 0.2952+j0.7423 & 0.04622+j0.2882 \\ 0.04620+j0.2448 & 0.04622+j0.2882 & 0.2952+j0.7423 \end{pmatrix}$$

REFERENCES

[1] H. Hu, Z. He, K. Wang, X. Ma and S. Gao, "Power-quality impact assessment for high-speed railway associated with high-speed trains using train timetable—part II: verifications, estimations and applications," *IEEE Trans. on Power Del.*, vol. 31, no. 4, pp. 1482-1492, Aug. 2016.

[2] J. C. Dai, X. Yang, L. Wen, "Development of wind power industry in china: a comprehensive assessment," *Renewable and Sustainable Energy Reviews*, vol.97, pp. 156-164, Dec. 2018.

[3] L. Li, X. Ren, Y. Yang, and *et al*, "Analysis and recommendations for onshore wind power policies in China," *Renewable and Sustainable Energy Reviews*., vol. 82, part. 1. pp. 156-167, Feb. 2018.

[4] "Feasibility Study Report on the Second Double Line of Lanzhou-Xinjiang Railway," China Railway Corp., Beijing, China 2009.

[5] U. Jayatunga, S. Perera, P. Ciufo, and A. P. Agalgaonkar, "A refined general summation law for VU emission assessment in radial networks," *Int. Jour. of Electr. Power and Energy Syst.*, vol. 73, pp. 329-339, Dec. 2015.

[6] L. F. L. Arão, A. L. F. Filho and M. V. B. Mendonça, "Comparative evaluation of methods for attributing responsibilities due to voltage unbalance," *IEEE Trans. on Power Del.*, vol. 31, no. 2, pp. 743-752, April 2016.

[7] "IEC/TR 61000-3-13", *Electromagnetic compatibility (EMC) – limits – assessment of emission limits for the connection of unbalanced installations to MV, HV and EHV power systems*, 2008.

[8] *The grid code, issue 5, revision 21*, 2017.

[9] "AS/NZS 61000-3-13", *Electromagnetic compatibility (EMC) - Part 3.13 Limits - Assessment of emission limits for the connection of unbalanced installations to MV, HV and EHV power systems*, 2012.

[10] *Eknisk forskrift 3.4.1 – Elforbrugende anlæg tilsluttet over 100 kV*, 2013.

[11] D. Perera, P. Ciufo, L. Meegahapola, and S. Perera, "Attenuation and propagation of voltage unbalance in radial distribution networks," *Int. Trans. on Electr. Energy Syst.,* vol. 25, pp. 3738-3752, March, 2015.

[12] CIGRE/CIRED working group C4.109, "CIGRE report 468–Review of Disturbance Emission Assessment Techniques,", ISBN: 978-2-85873-158-9, 2011.

[13] E. C. Quispe and I. D. Lopez, "Effects of unbalanced voltages on the energy performance of three-phase induction motors," *2015 IEEE Workshop on Power Electronics and Power Quality Applications (PEPQA)*, Bogota, 2015, pp. 1-6.

[14] A. P. G. J. Vinicius P. Suppioni, "Improving network voltage unbalance levels by controlling DFIG wind turbine using a dynamic voltage restorer," *Int. Jour. of Electr. Power & Energy Syst.,* vol. 96, pp. 185-193, March, 2018.

[15] L. Xu and Y. Wang, "Dynamic modeling and control of DFIG-based wind turbines under unbalanced network conditions," *IEEE Trans. on Power Syst.*, vol. 22, no. 1, pp. 314-323, Feb. 2007.

[16] Yaw-Juen Wang, "Analysis of effects of three-phase voltage unbalance on induction motors with emphasis on the angle of the complex voltage unbalance factor," *IEEE Trans. on Energy Convers.*, vol. 16, no. 3, pp. 270-275, Sept. 2001.

[17] A. B. F. Neves, A. d. L. F. Filho and M. V. B. de Mendonça, "Effects of voltage unbalance on torque and efficiency of a three-phase induction motor," *2014 16th Int.l Conf. on Harmonics and Quality of Power (ICHQP)*, Bucharest, 2014, pp. 679-683.

[18] H. Nian, T. Wang and Z. Q. Zhu, "Voltage imbalance compensation for doubly fed induction generator using direct resonant feedback regulator," *IEEE Trans. on Energy Convers.*, vol. 31, no. 2, pp. 614-626, June 2016.

[19] M. Savaghebi, A. Jalilian, J. C. Vasquez and J. M. Guerrero, "Autonomous voltage unbalance compensation in an islanded droop-controlled microgrid," *IEEE Trans. on Ind. Electron.*, vol. 60, no. 4, pp. 1390-1402, April 2013.

[20] Q. Xu, F. Ma, Z. He and *et al*., "Analysis and Comparison of Modular Railway Power Conditioner for High-Speed Railway Traction System," in *IEEE Transactions on Power Electronics*, vol. 32, no. 8, pp. 6031-6048, Aug. 2017.

[21] T. Wang, H. Nian, Z. Q. Zhu, L. Ding and B. Zhou, "Flexible Compensation Strategy for Voltage Source Converter Under Unbalanced and Harmonic Condition Based on a Hybrid Virtual Impedance Method," in *IEEE Transactions on Power Electronics*, vol. 33, no. 9, pp. 7656-7673, Sept. 2018.

[22] N. Dai, M. Wong, K. Lao and C. Wong, "Modelling and control of a railway power conditioner in co-phase traction power system under partial compensation," in *IET Power Electronics*, vol. 7, no. 5, pp. 1044-1054, May 2014.

[23] M. Chen, Q. Li, C. Roberts and *et al*., "Modelling and performance analysis of advanced combined co-phase traction power supply system in electrified railway," in *IET Generation, Transmission & Distribution*, vol. 10, no. 4, pp. 906-916, 10 3 2016.

[24] P. Paranavithana and S. Perera, "A robust voltage unbalance allocation methodology based on the IEC/TR 61000-3-13 guidelines," *2009 IEEE Power & Energy Society General Meeting*, Calgary, AB, 2009, pp. 1-6.

[25] D. Perera, P. Ciufo, L. Meegahapola, and S. Perera, "Attenuation and propagation of voltage unbalance in radial distribution networks," *Int. Trans. on Electr. Energy Syst.,* vol. 25, pp. 3738-3752, March, 2015.

Yinyu Chen (S'18) received the B.Eng. degree in electrical engineering from the Kunming University of Science and Technology, Kunming, China, in 2017. He is currently working toward the M.S. degree in electrical engineering from Southwest Jiaotong University, Chengdu, China. His current research interests include railway traction system and power quality assessment and control.

Minwu. Chen (M'17) received the B.Eng. and Ph.D. degrees in electrical engineering from the Southwest Jiaotong University, Chengdu, China, in 2004 and 2009, respectively.

From 2010 to 2012, he was a Postdoctoral with the China Railway First Survey and Design Institute Group, Xi'an, China. Since 2012, he has been an Associate Professor in the College of Electrical Engineering, Southwest Jiaotong University, Chengdu, China. From the 2014 to 2015, he was a Visiting Scholar in the University of Birmingham, Birmingham, U.K. His research interests include new technology and power quality for railway traction system.

Zhongbei Tian received the B.Eng. degree from the Huazhong University of Science and Technology, Wuhan, China, in 2013, and the B.Eng. and Ph.D. degrees in electrical and electronic engineering from the University of Birmingham, Birmingham, U.K., in 2013 and 2017, respectively. He is currently a Research Fellow with the University of Birmingham. His research interests include railway traction system and power network modeling, energy systems optimization, advanced power systems design, and the analysis of electric railways.

Yuanli Liu received the B.Eng. degree in electrical engineering from the Southwest Jiaotong University, Chengdu, China, in 2017, where he is currently working toward the M.S. degree in electrical engineering. His research interests include railway power traction system, renewable energy and energy storage systems.